EUCASS 2025 ROME, ITALY (PAPER 598)

SIDE LOAD REDUCTION OF HIGH AREA RATIO NOZZLES

CHARLES E. TINNEY
JOHN VALDEZ
APPLIED RESEARCH LABORATORIES, UT AUSTIN

JOSEPH RUF
TRAVIS RIVORD
MARSHALL SPACE FLIGHT CENTER, NASA
email: charles.tinney@arlut.utexas.edu

scan me!

Overview

charles.tinney@arlut.utexas.edu

Nozzle side loads during startup are driven by shock foot asymmetries

1. FSS->RSS transition
2. EER (end effects regime)

- Foster and Cowles (1949) Experimental study of gas-flow separation in overexpanded exhaust nozzles for rocket motors. NASA PR-N3-103

- Stark, Genin (2011,2016) side load reduction device
- Hadjadj Perrot, Verma (2015) film cooling
- Ivanov, Kryukov (2019) wall vents
- Legros et al (2022) dual-bell nozzles

- No new launch debris
- Currently avoiding significant changes to nozzle contour or other mission critical hardware
- Nozzle must pass certification process.

Free Shock Separated Flow (FSS)

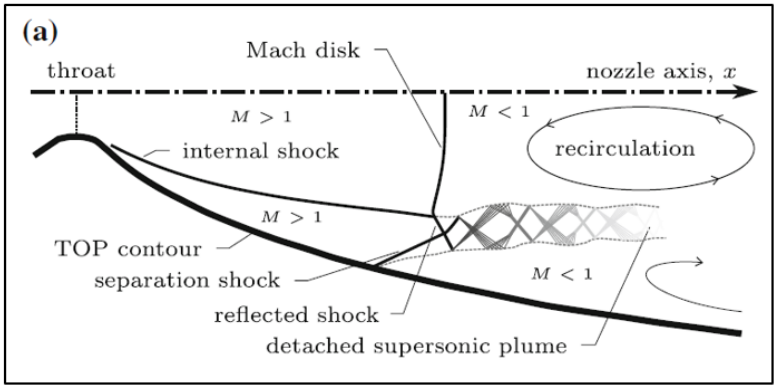

Restricted Shock Separated Flow (RSS)

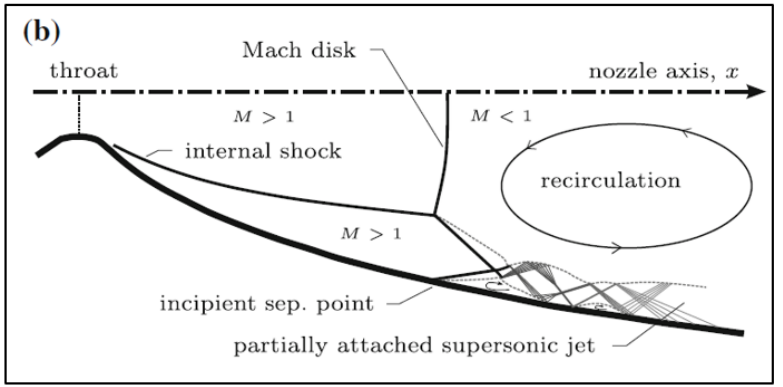

Source: Baars & Tinney (2013), Exp. Fluids Vol. 54, No. 1468

Experimental Setup

charles.tinney@arlut.utexas.edu

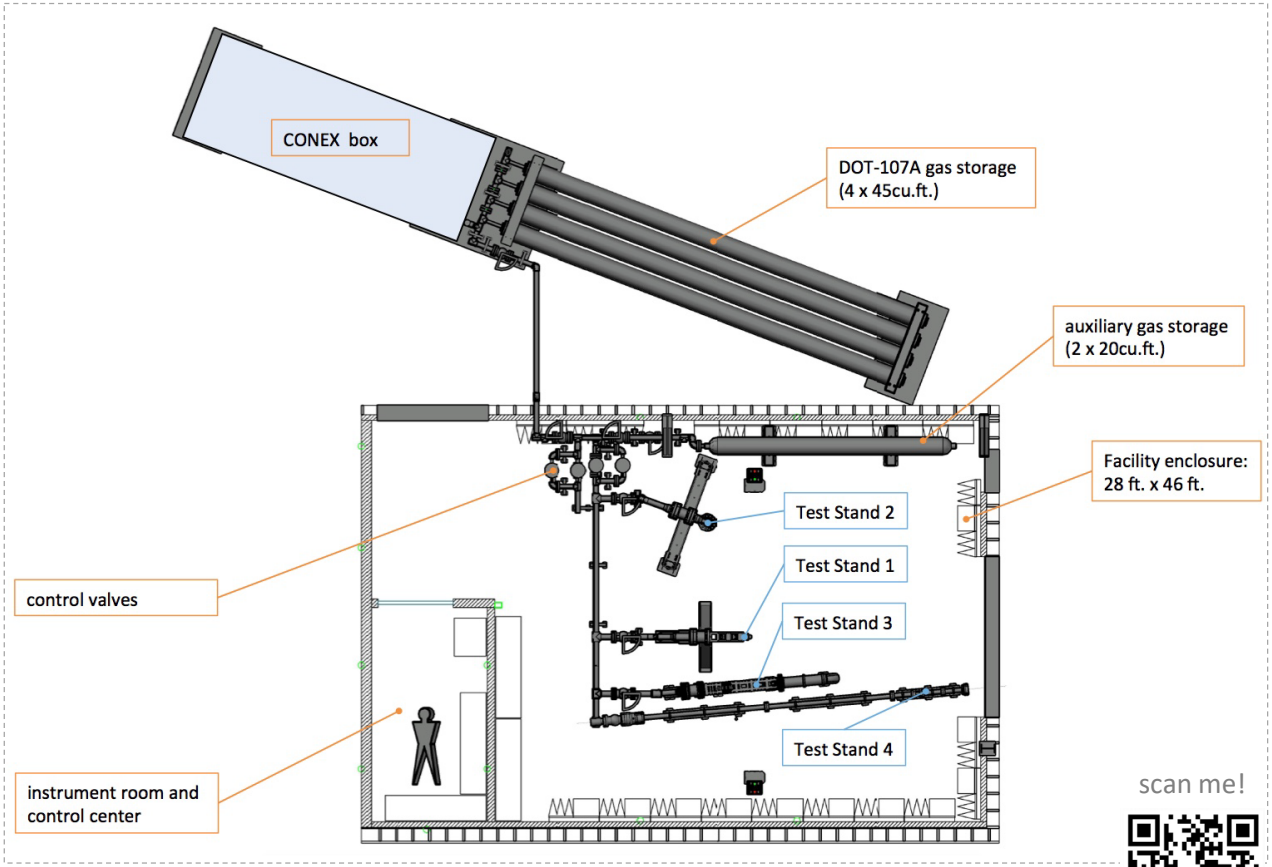

scan me!

Experimental Setup

charles.tinney@arlut.utexas.edu

Nozzle Side Load Sensing System

- Flow through type strain tube method
- Two orthogonal strain gauge pairs
- Temperature compensated
- Pressure compensated to within ~%5

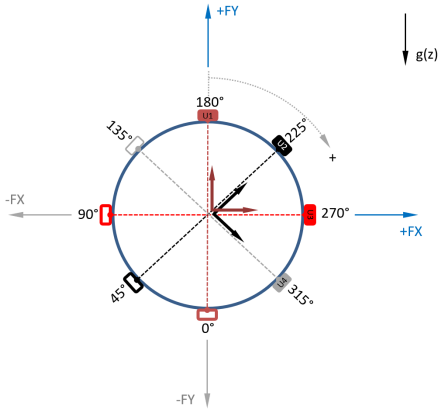

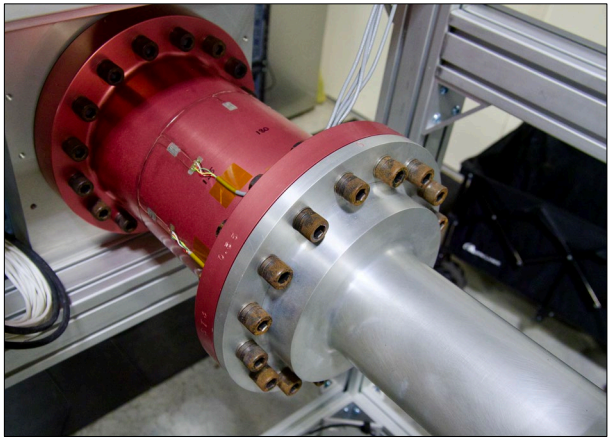

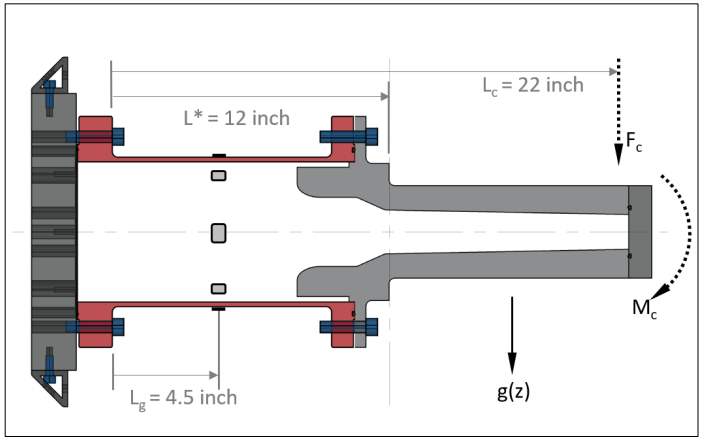

Experimental Setup

charles.tinney@arlut.utexas.edu

Nozzle Side Load Sensing System

- Flow through type strain tube method
- Two orthogonal strain gauge pairs
- Temperature compensated
- Pressure compensated to within ~%5

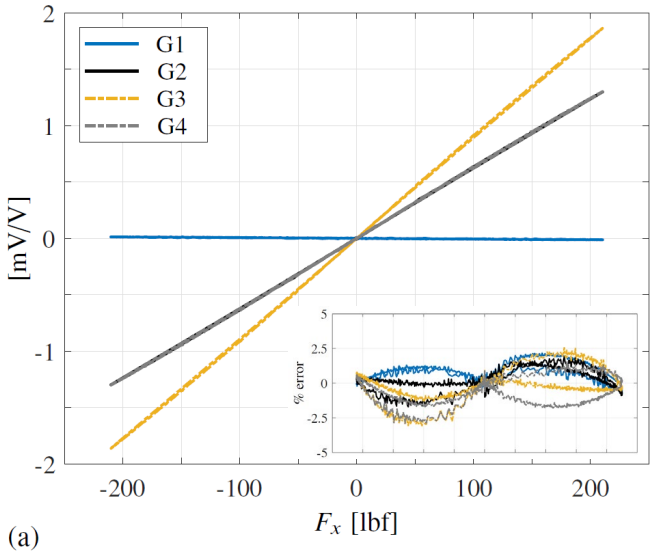

(a)

Expressions for performing the second order calibration are as follows. We begin by generating second order expressions using least squares regression to independently relate the x-direction force f_x to sensor voltages v_1 and v_2 by way of f_{x1} and f_{x2}, respectively.

$$f_{x1} = \left(a_{x1}v_1^2 + b_{x1}v_1 + c_{x1}\right) \tag{19}$$

$$f_{x2} = \left(a_{x2}v_2^2 + b_{x2}v_2 + c_{x2}\right) \tag{20}$$

In theory, if $v1 \neq 0$ and $v_2 \neq 0$ when $f_x \neq 0$, then $f_{x1} = f_{x2}$. Expressions relating the y-direction force to sensor voltages v_1 and v_2 are defined identically as follows,

$$f_{y1} = \left(a_{y1}v_1^2 + b_{y1}v_1 + c_{y1}\right) \tag{21}$$

$$f_{y2} = \left(a_{y2}v_2^2 + b_{y2}v_2 + c_{y2}\right) \tag{22}$$

$$[W_b] = \begin{bmatrix} b_{x1}^{-1} & b_{x2}^{-1} \\ b_{y1}^{-1} & b_{y2}^{-1} \end{bmatrix}; \qquad [W_b]^{-1} = [W_B] = \begin{bmatrix} B_{x1} & B_{x2} \\ B_{y1} & B_{y2} \end{bmatrix} \tag{23}$$

$$[W_a] = \begin{bmatrix} a_{x1}^{-1} & a_{x2}^{-1} \\ a_{y1}^{-1} & a_{y2}^{-1} \end{bmatrix}; \qquad [W_a]^{-1} = [W_A] = \begin{bmatrix} A_{x1} & A_{x2} \\ A_{y1} & A_{y2} \end{bmatrix} \tag{24}$$

where $[W_b]$ and $[W_a]$ are the first and second order polynomial coefficient matrices, respectively, while $[W_B]$ and $[W_A]$ are their corresponding inverse, so that $[W_b][W_B] = [I]$ and $[W_a][W_A] = [I]$. It follows then that

$$F_x = \left(A_{x1}v_1^2 + B_{x1}v_1 + C_{x1}\right) + \left(A_{x2}v_2^2 + B_{x2}v_2 + C_{x2}\right) \tag{25}$$

$$F_y = \left(A_{y1}v_1^2 + B_{y1}v_1 + C_{y1}\right) + \left(A_{y2}v_2^2 + B_{y2}v_2 + C_{y2}\right) \tag{26}$$

$$\begin{bmatrix} F_x \\ F_y \end{bmatrix} = \begin{bmatrix} A_{x1} & A_{x2} \\ A_{y1} & A_{y2} \end{bmatrix} \begin{bmatrix} v_1^2 \\ v_2^2 \end{bmatrix} + \begin{bmatrix} B_{x1} & B_{x2} \\ B_{y1} & B_{y2} \end{bmatrix} \begin{bmatrix} v_1 \\ v_2 \end{bmatrix} + \begin{bmatrix} C_{x1} & C_{x2} \\ C_{y1} & C_{y2} \end{bmatrix} \tag{27}$$

$$[F] = [W_B]^{-1}[V] + [W_A]^{-1}[V]^2 \tag{28}$$

Experimental Setup

charles.tinney@arlut.utexas.edu

Thrust Optimized Parabolic (TOP) contour

- Ruf et al. (2009) AIAA Paper 2009-4859
  - $A/A^* = 30.29$
  - $r_c = r^*$
  - $\alpha_c = 40$ deg (throat)
  - $\alpha_e = 7$ deg (exit)

Instruments:

- Nozzle sideloads (2kHz sample rate)
- P-static, 32 channels (500 Hz)
- P-dynamic, kulite (20 kHz)

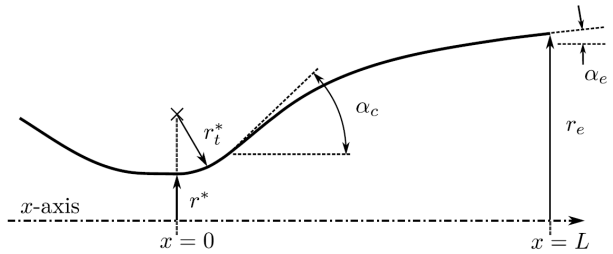

Donald et al. (2014), AIAA Journal. Vol. 52, No. 7

no.	nozzle	x_L [inch]	D^* [inch]	D_e [inch]	material	surface [μm]	kulite	P-wall	loads
1	smooth-wall (large)	9.375	1.5	8.255	AL-6061	20 - 40	—	●	—
2	smooth-wall (small)	3.125	0.5	2.752	AL-6061	0.1 - 0.4	●	●	●
3	rough-wall	3.125	0.5	2.752	SLSN	40	●	●	●
4	ported-wall	3.125	0.5	2.752	SLSN	40	●	●	●
5	tare	3.125	0.5	0.402	SLSN	40	—	—	●

Table 1: **Summary of nozzle hardware tested.**

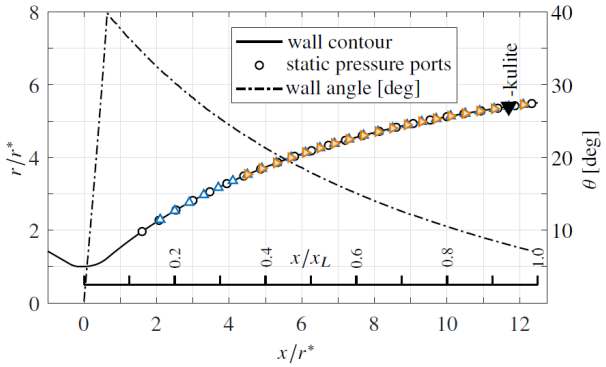

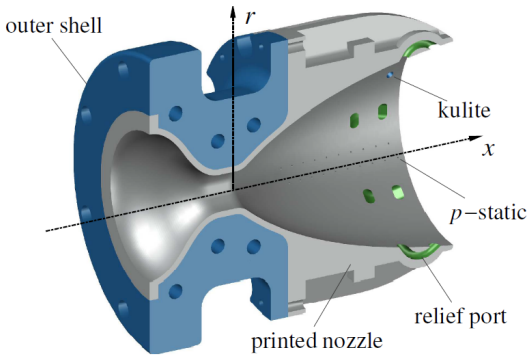

Figure 1: (a) Thrust optimized parabolic nozzle contour with wall angle [deg] and location of static pressure sensing ports for the different nozzles. (b) Cross-section of additive manufactured rough-wall nozzle and its major components.

Experimental Setup

charles.tinney@arlut.utexas.edu

Thrust Optimized Parabolic (TOP) contour

- Ruf et al. (2009) AIAA Paper 2009-4859
  - $A/A^* = 30.29$
  - $r_c = r^*$
  - $\alpha_c = 40$ deg (throat)
  - $\alpha_e = 7$ deg (exit)

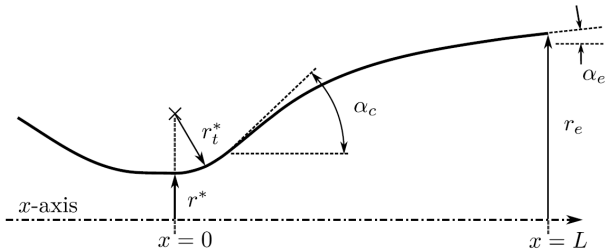

Donald et al. (2014), AIAA Journal. Vol. 52, No. 7

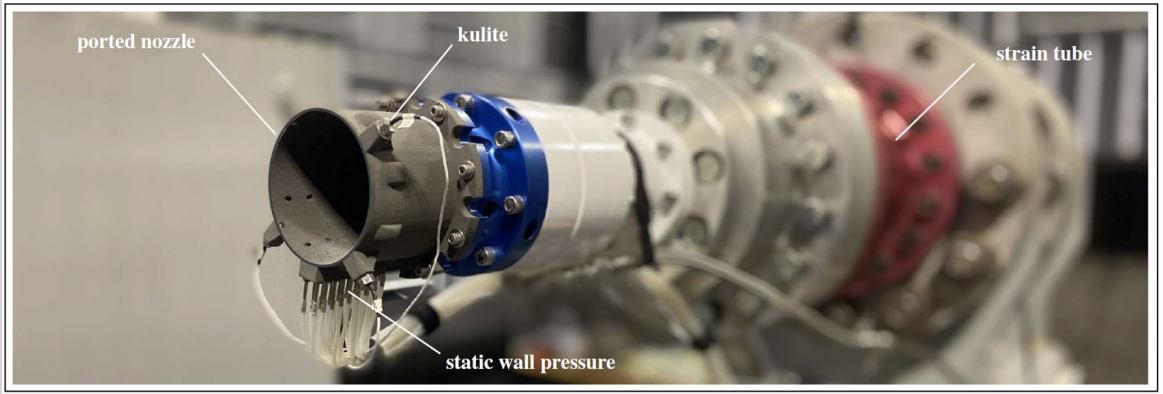

Figure 2: Image of the ported-wall nozzle during testing.

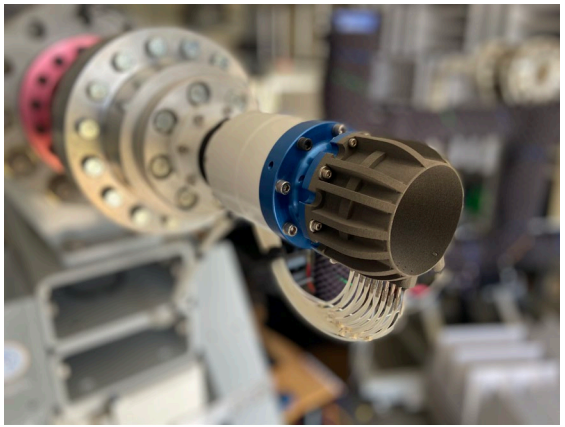

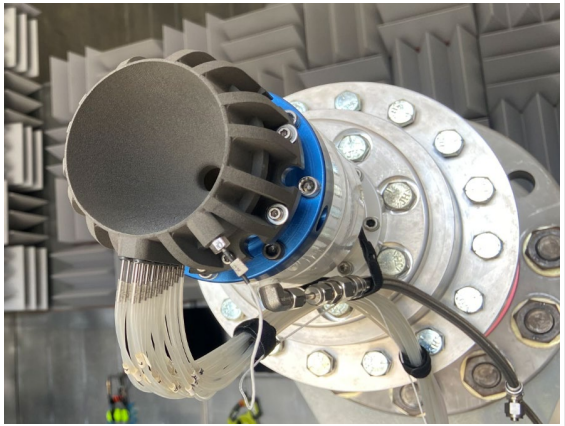

Results

charles.tinney@arlut.utexas.edu

Testing practices

- 10 tests: Tare
- 25 tests/nozzle: Smooth, Rough-, Ported-wall

no.	nozzle	x_L [inch]	D^* [inch]	D_e [inch]	material	surface [μm]	kulite	P-wall	loads
1	smooth-wall (large)	9.375	1.5	8.255	AL-6061	20 - 40	—	●	—
2	smooth-wall (small)	3.125	0.5	2.752	AL-6061	0.1 - 0.4	●	●	●
3	rough-wall	3.125	0.5	2.752	SLSN	40	●	●	●
4	ported-wall	3.125	0.5	2.752	SLSN	40	●	●	●
5	tare	3.125	0.5	0.402	SLSN	40	—	—	●

Table 1: **Summary of nozzle hardware tested.**

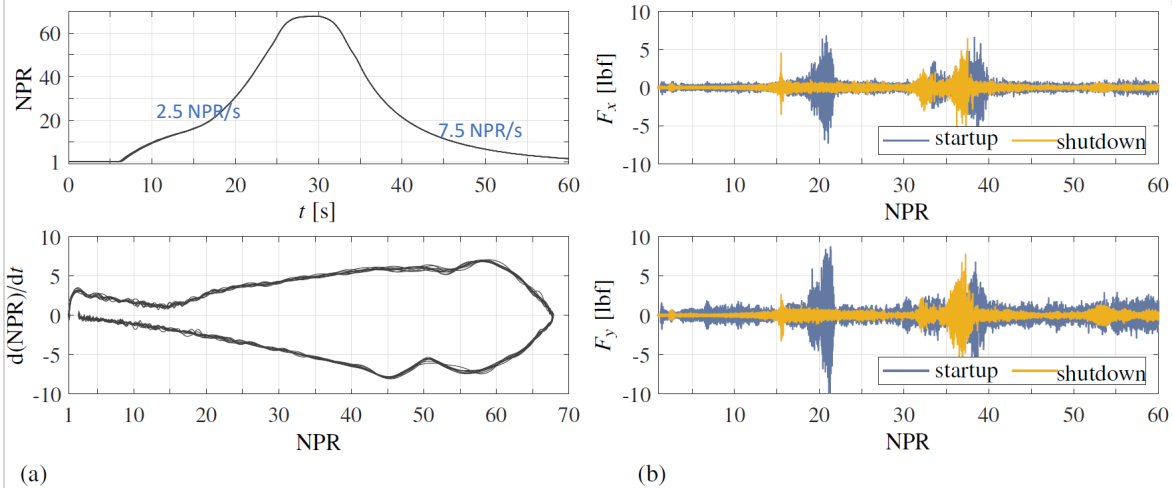

Figure 6: (a) Nozzle pressure ratio and its time derivative during testing. (b) sample nozzle side-loads during startup and shut down.

Results

charles.tinney@arlut.utexas.edu

P-static

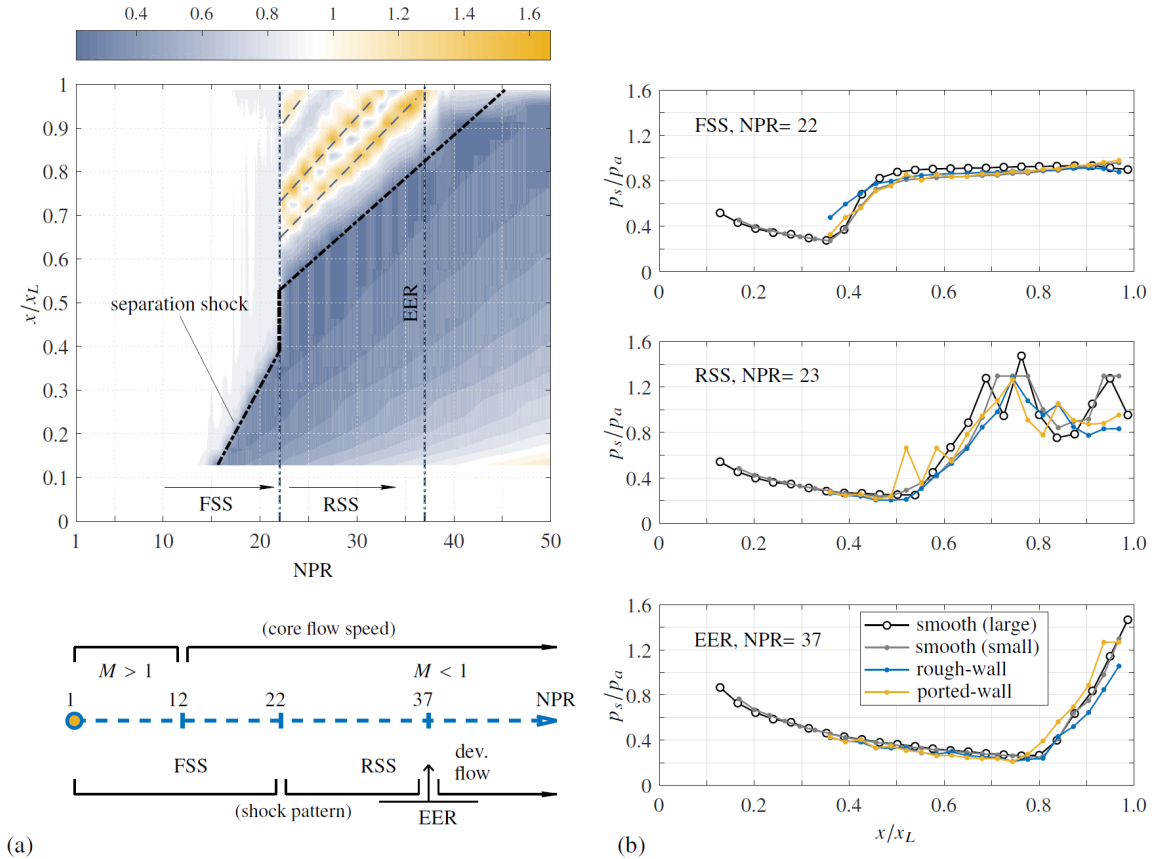

Figure 7: a) Static wall pressure (p_s/p_a) during startup of the large, smooth-wall TOP nozzle. b) Comparison of static wall pressures (p_s/p_a) corresponding to FSS, RSS and EER flow states of all TOP nozzles.

Results

charles.tinney@arlut.utexas.edu

P-dynamic

- Peak pressures during EER:
  - Smooth wall: 183.6 dB
  - Rough wall: 173.5 dB (-10dB)
  - Ported wall: 168.6 dB (-15dB)

- Peak to Valley Pressure range during EER
  - Smooth wall: 1.30 atm
  - Rough wall: 0.50 atm
  - Ported wall: 0.32 atm

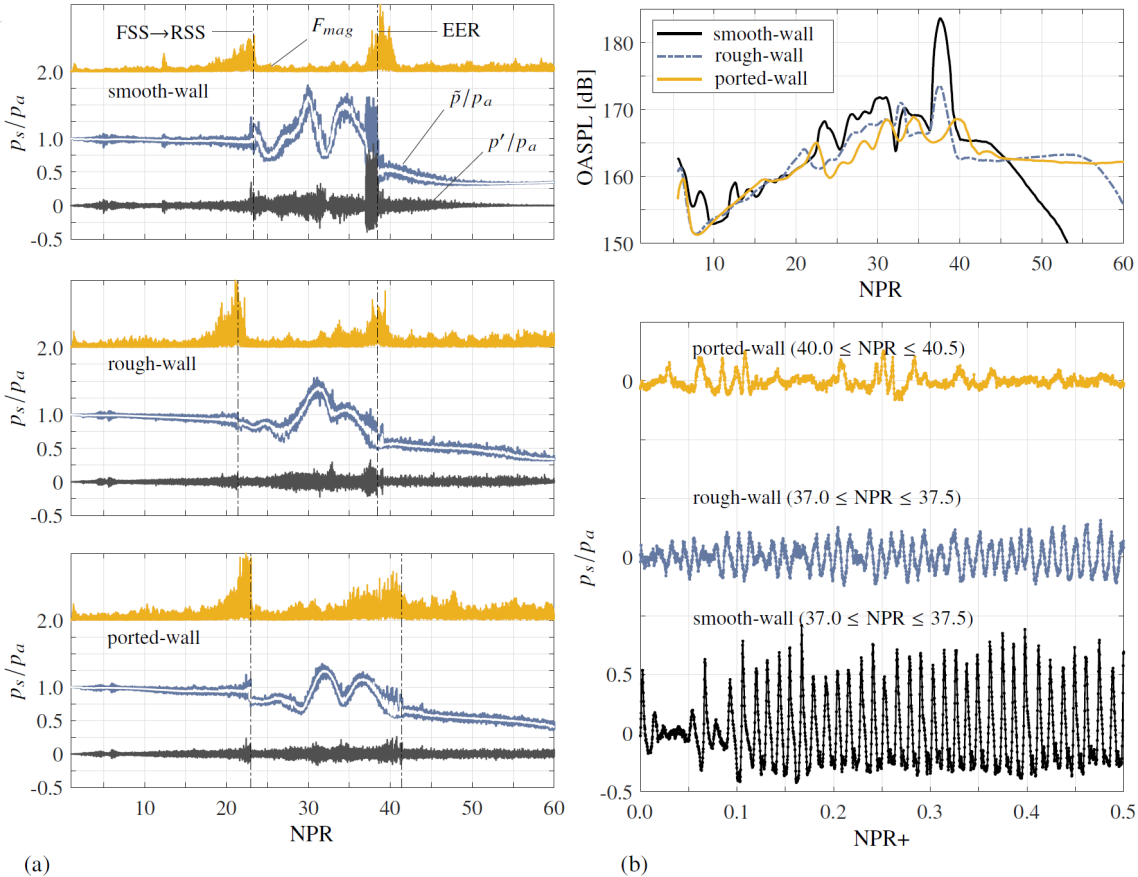

Figure 8: (a) Kulite pressure reading during startup and overall sound pressure level [dB] of all tests for the small-TOP nozzle, (b) Pressure time series during end-effects for all small nozzles.

Results

P-dynamic

- Peak pressures during EER:
  - Smooth wall: 156.8 dB at 370 Hz at NPR 37.6
  - Rough wall: 146.6 dB at 425 Hz at NPR 37.4
  - Ported wall: no EER tone

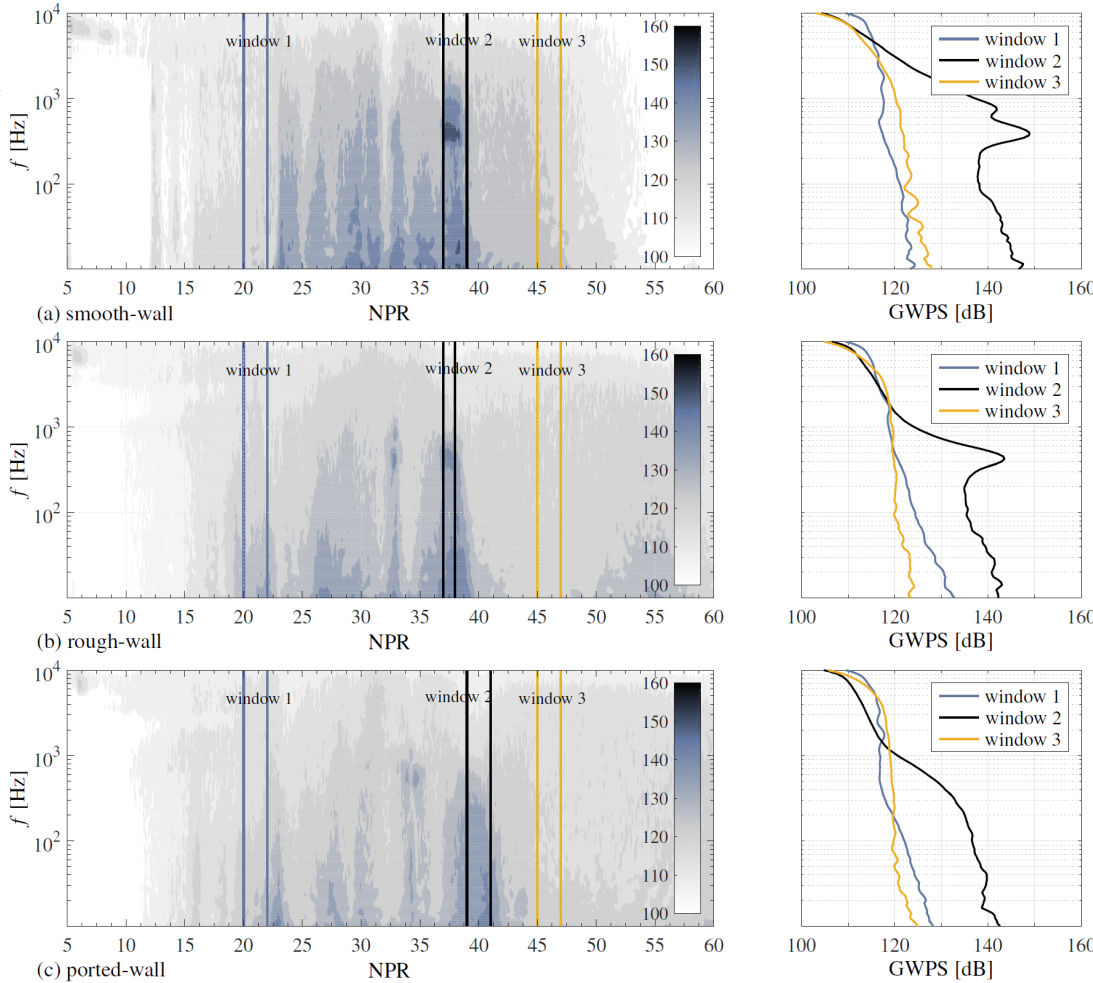

Figure 9: Wavelet power spectra [dB] of the unsteady lip pressure during startup of the (a) smooth-wall, (b) rough-wall, and (c) ported-wall nozzles. Global Wavelet Power Spectra [dB], averaged over the three windows identified in the WPS.

Results

- Nozzle Side Loads

No.	nozzle	(FSS→RSS) NPR	(FSS→RSS) F_{mag} [lbf]	(EER) NPR	(EER) F_{mag} [lbf]
2	smooth-wall	22.25	8.55	38.75	15.10
3	rough-wall	21.25	17.26	38.75	9.18
4	ported-wall	21.75	11.95	40.25	6.34
5	tare	20.75	1.34	38.25	1.98

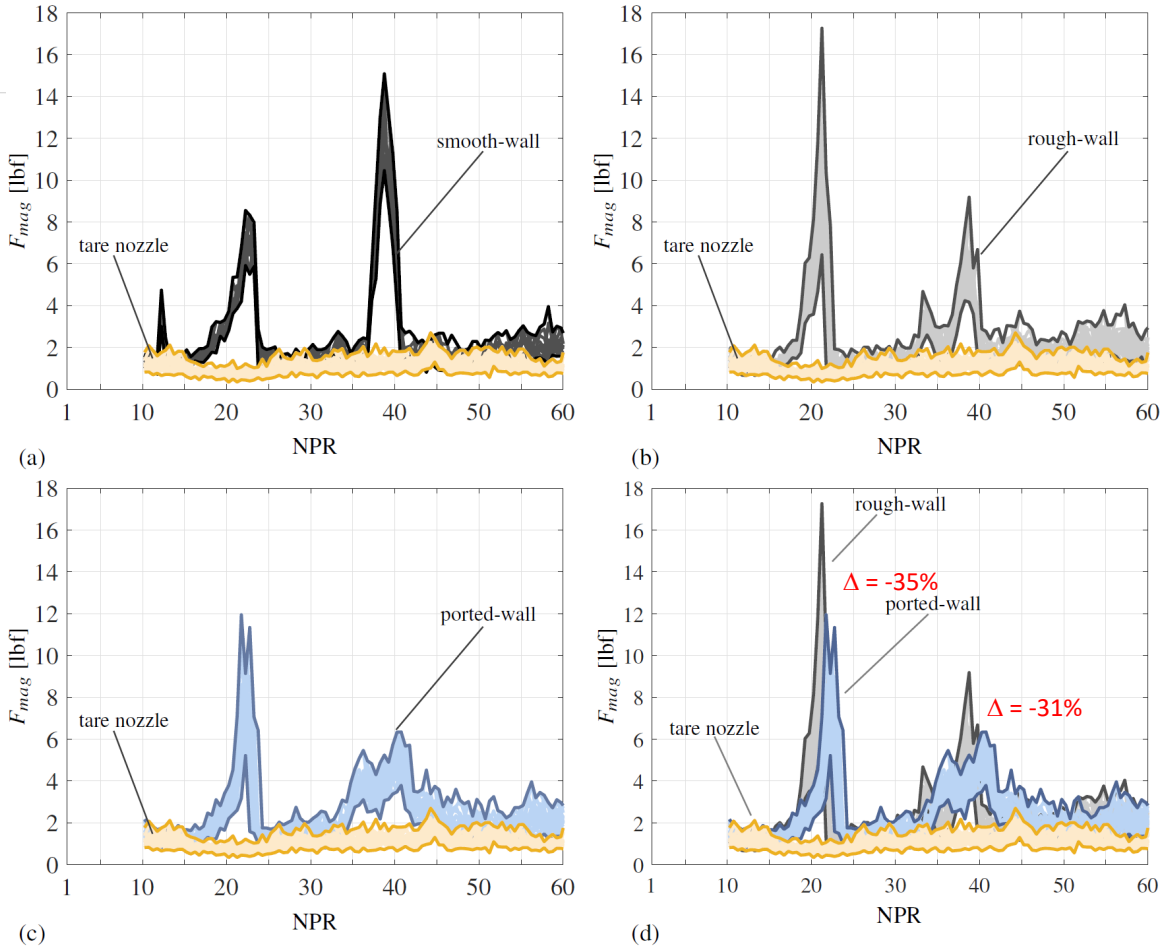

Figure 10: Maximum and minimum force magnitude (F_{mag}) side-loads recorded by the (a) smooth-wall, (b) rough-wall, and (c) ported-wall nozzles during startup. (d) Comparison between rough-wall and ported-wall nozzles.

Come find us

charles.tinney@arlut.utexas.edu

Burdairon, Blanchard, Tinney, Daviller, (2025) Large Eddy Simulation of a Rocket Nozzle Undergoing End Effects.

Room H, Prophy 20: Tuesday, July 1, 9:00am (paper 28)

11th EUROPEAN CONFERENCE FOR AERONAUTICS AND AEROSPACE SCIENCES (EUCASS)

DOI: ADD DOINUMBER HERE 00000000

Large-Eddy Simulation of a Rocket Nozzle Undergoing End Effects

*F. Burdairon**†, S. Blanchard°, C. E. Tinney°, G. Daviller**
°*CNES - 52, Rue Jacques Hillaires, 75612 PARIS Cedex - FRANCE*
°*The University of Texas at Austin, Austin, Texas 78713 - USA*
**CERFACS - 42 av. G. Coriolis 31057 Toulouse Cedex 01 - FRANCE*
burdairon@cerfacs.fr · simon.blanchard@cnes.fr · daviller@cerfacs.fr · charles.tinney@arlut.utexas.edu
†Corresponding author

Abstract

TO BE WRITE *The aim of this study is to investigate the End-Effects Regime for a thrust-optimized parabolic (TOP) nozzle contour [1] through Large-Eddy Simulation (LES). The AVBP compressible solver is employed .... The TOP nozzle is characterized by a design Mach number of $M_d = 5.24$ and an exit-to-throat area ratio of $A_1/A^* = 30.29$. The EER occurs at $NPR = 37$. After validating the LES results against experimental data (static wall pressure and Schlieren images), the EER is analyzed.*

1 Introduction

During ignition and extinction of their engines, space vehicle propulsion systems are subjected to significant side loads. In the internal flow inside the nozzle, a separation can appear through interaction between the shock pattern and the boundary layer, which leads to different flow regimes depending on the nozzle geometry and the Nozzle Pressure Ratio (NPR, the ratio between the inlet and ambient pressures). At ignition, the flow experiences Free-Shock Separation (FSS) (add description). As the NPR increases, the flow transitions to a Restricted Shock Separation (RSS) (add description). In the RSS regime, the boundary layer reattaches to the nozzle wall, and the flow exhibits a series of trapped annular recirculating bubbles, whose locations depend on the NPR. There is a critical NPR range where the most downstream bubble is close enough to the lip so that it opens up intermittently to the ambient air. This is the so-called End-Effects Regime (EER) as described by Nave and Coffey [2]. The strong asymetries in the shock foot then produce significant side loads on the nozzle, which are propagated to the vehicle and its payload. Understanding and mitigating the EER is therefore essential when designing nozzles to optimize rocket performance under various flight conditions.

The aim of this study is to investigate the EER event using high fidelity simulations, specifically through Large-Eddy Simulation (LES), for a high area ratio nozzle. The retained configuration relies on a thrust-optimized parabolic (TOP) contour, which has been experimentally studied ([3] [1] [4] [5] [1]), and is known to experiences FSS, RSS and EER regimes. The design Mach number is $M_d = 5.24$, the exit-to throat area ratio is $A_1/A^* = 30.29$, and the EER begins at $NPR = 37$, up to 39.

2 Configuration

The thrust optimized parabolic nozzle used for this study is the one designed by Ruf et al. (2009) [6] and has been shown to generate both FSS and RSS flow states, followed by an EER event at relatively low nozzle pressure ratios. The nozzle shape is shown in Fig. 1a alongside a CAD rendering in Fig. 1b and has a throat diameter of $D^* = 12.7$ mm, and a nozzle length (measured from the throat curvature to the nozzle lip) of $x_L = 79.375$ mm. The exit diameter is valued at $D_e = 69.9$ mm resulting in an area ratio of $A_e/A^* = 30.3$. This corresponds to a design Mach number of 5.24 and would be achieved with a pressure ratio of 700. This particular nozzle has been studied extensively over the years by Canchero et al. (2016) [5] and Rojo et al. (2016) [1], and is a truncated version of the nozzle reported by Baars et al. (2012) [7], and Martelli et al. (2020) [8].

scan me!